A Web-Based Georeferenced Model of the Urban Traction Electrification System in Turin

A Web-Based Georeferenced Model of the Urban Traction Electrification System in Turin

Pietro Colella, *Member, IEEE*, and Enrico Pons, *Senior Member, IEEE*

***Abstract*—Transport accounts for approximately 25% of Green House Gas emissions in Europe, with urban road transport being a major contributor to air pollution. Decarbonizing urban transport is essential, particularly as over 70% of Europeans reside in urban areas. Strengthening public transport, the most sustainable travel option for large populations, is a key strategy. This article focuses on urban tramways, formed by the urban traction electrification systems and electric public transport vehicles. A digital twin approach is proposed to improve the operational activities of tramways, aiming to optimize system design, enhance maintenance, improve reliability, and unlock unused infrastructure potential, such as using the tramway infrastructure for off-peak charging stations. This article presents the methodology adopted to develop the model of the tramway in Turin, Italy. This step is a milestone to implement the tramway digital twin. Moreover, this article presents the validation process of the model, which was carried out through a comparison with both simulated and field measurement data.**

***Index Terms*—Digital twin (DT), model, traction electrification system, tramway.**

Nomenclature

DT	Digital twin.
EPTV	Electric public transport vehicle.
GTT	Gruppo Torinese Trasporti.
OCS	Overhead contact system.
TTN-S	turin tram network simulator.
UTES	Urban traction electrification systems.

I. Introduction

TRANSPORT contributes by almost 25% to the total green house gas emissions in Europe and is the main cause of air pollution in cities. Since more than 70% of European citizens live in urban areas, decarbonizing urban road transport is mandatory to reduce emissions in this sector. Several actions have been planned to reach the goal. One is promoting and strengthening public transport, considering that it represents the safest, most efficient, and sustainable way for large numbers of people to travel [1].

This article is focused on a specific sector of urban public transport, i.e., the urban tramway, which is composed of an electric infrastructure and electric vehicles. The first system, referred to as the UTES, is typically supplied by substations equipped with power transformers, ac–dc converters, protective relays, and circuit breakers. These substations use multiple dc feeders (positive cables) to supply power to the OCS, while the return current is collected through the rails and negative cables [2]. A UTES can feed several types of EPTVs, differing from power traction technology and energy consumption.

A method to improve a public tramway is the implementation of its DT, which can be defined as a comprehensive digital representation of a system through models and data [3], [4]. The DT of an urban tramway is formed by two building blocks: the model of the UTES and the model of the running EPTV. More specifically, the model of the UTES shall be designed to receive data from sensors installed on board the EPTV and on crucial points of the infrastructure (such as the substations): the first ones provide the exact location of the vehicle, the voltage measured at the pantograph, and the absorbed current; the second ones could be useful for monitoring the operating status of the equipment [5], [6]. Additional layers can be added to monitor quantities of interest, such as the number of passengers on the vehicles, the presence of ice on the OCS, and the cable temperatures [7].

A DT that considers both UTESs and EPTVs would support the public transport companies in several aspects, such as the following:

1) the support in the designing and operation activities;
2) the reduction of the UTES and EPTV out-of-service using predictive maintenance algorithms [8], [9];
3) the identification of alternative UTES configurations to improve the performance on specific aspects, such as reducing the energy losses or increasing the reliability;
4) the possibility of training operators using real scenarios;
5) the valorization of the UTES, which is often used only to feed EPTVs, such as trams and trolley buses. During the night or outside peak hours, the network is used below its potentiality. Reliable models can quantify these situations, supporting the implementation of different strategies to take a larger benefit from the infrastructure. For instance, in certain areas, the UTES could feed some electric vehicle charging stations [10], [11].

Received 4 September 2025; revised 5 December 2025; accepted 11 December 2025. This work was supported by the “DC smart grids for Next generation Transportation Systems (NeTS)” project—funded by European Union—Next Generation EU within the PRIN 2022 program (D.D. 104—2 February 2022 Ministero dell’Università e della Ricerca). Paper no. TII-25-6048. *(Corresponding author: Pietro Colella.)*

The authors are with the Department of Energy “Galileo Ferraris,”, Politecnico di Torino, 10129 Torino, Italy (e-mail: pietro.colella@polito.it; enrico.pons@polito.it).

Digital Object Identifier 10.1109/TII.2025.3644646

TABLE I
FEATURE COMPARISON OF TRACTION-POWER TOOLS

Feature	TNN-S (this work)	eTraX (ETAP) [14]	FABEL (Enotrac) [15]	OpenPowerNet (OpenTrack Railway Tech.) [16]	Sidytrac (Siemens) [17]	SIGNON Suite (SIGNON) [18]	TTS/SIMON PowerLog (ÅF-Industriteknik) [19]
Flexible Autodesk import (attribute mapping)	✓	✗	✗	✗	✗	✗	✗
Suitability for Digital Twin applications	✓	✗	✗	✗	✓	✗	✗
Support for operating and fault scenario modeling	✓	✓	✓	✓	✓	✓	✓
Support for integrating ad-hoc code (user scripting/API)	✓	✓	✓	✗	✓	✗	✗
Availability as a web-based application	✓	✓	✗	✗	✓	✗	✗
Compatibility with multiple platforms (OS)	✓	✓	✗	✗	✓	✗	✗
Geospatial data management and view	✓	✓	✓	✗	✗	✓	✗

Legend: ✓ = documented support; ✗ = unavailable or not clearly documented.

This article focuses on the first constitutive block of the DT, which concerns the modeling of the UTES. The main objective is to provide a systematic and rigorous account of the methodology employed to develop and implement the UTES model for the city of Turin, Italy, which is conceived as a fundamental step toward the implementation of its tramway DT. The case study in Turin was carried out in cooperation with GTT and Infra.To—Infrastrutture per la Mobilità [12], [13], which manage the public transport fleet and the transport infrastructure, respectively. It provides a concrete application that exemplifies how the proposed methodology can be effectively employed in a real urban context.

These companies manage the public transport fleet and the transport infrastructure, respectively.

The requirements for the application are as follows:

1) the UTES model shall be developed based on its geometrical representation, given the original data format (Autodesk DWG file) and the advantage of drawing software, which enables quick and easy drafting of large network portions;
2) the UTES model shall be georeferenced;
3) the calculation of the currents and voltages shall be sufficiently fast to allow a quasi-real-time experience;
4) the position and the current absorbed by the vehicles can be provided manually by the User or received by on-field sensors.

Various commercial software tools are available for simulating railway power supply systems [14], [15], [16], [17], [18], [19], but none fully meet the above-mentioned requirements, as shown in Table I.

To the best of the authors' knowledge, the software tools currently available on the market do not provide the necessary functionalities to implement a DT of a tramway network for the purpose of conducting both electrical network and energy analyses. In particular, none of the existing platforms offers sufficiently flexible procedures for importing data from an Autodesk DWG file, a capability that is indispensable for addressing the high degree of coding complexity inherent in the tramway network of Turin. To make a model, it is necessary to develop it from scratch using their graphical user interface. A UTES is a complex network and this operation can be very time-consuming. Moreover, many commercial solutions lack robust support for the georeferenced management of infrastructure data and EPTVs, which is a critical requirement for accurate spatial modeling of large-scale urban transport systems. Finally, current software environments generally do not allow for the systematic integration of vehicle-level energy consumption data obtained from on-board smart meters, thereby preventing the establishment of a comprehensive and dynamically updated DT framework. In many cases, the tools are developed to model transient phenomena, which are not relevant to the considered application and instead significantly complicate the calculations, making it difficult to calculate currents and voltage in quasi-real-time.

For our purposes, representing a running vehicle as a sequence of steady-state events is sufficient, given that the primary interest lies in energy evaluation and grid steady-state analysis, rather than in vehicle dynamics.

Beyond fulfilling the design requirements outlined above, the proposed software provides a versatile platform with both scientific and industrial relevance. From a research perspective, it enables the development and testing of advanced optimization algorithms for network operation and energy management, as well as the implementation of predictive maintenance strategies to enhance system reliability. Furthermore, the framework allows for the investigation of emerging challenges such as the integration and charging impact of electric vehicles on the dc traction network, offering valuable insights into future scenarios of electrified urban mobility. From an industrial standpoint, the software constitutes a practical decision-support tool that can guide operators in improving efficiency, reducing operational risks, and supporting the transition towards more sustainable and resilient tramway infrastructures.

The rest of this article is organized as follows. Section II provides a concise overview of the UTES in Turin. Section III details the electrical models developed for each UTES component. Section IV introduces the nodal-analysis method in matrix form, which is employed to compute line currents and nodal voltages. Section V describes the implementation of the TTN-S, outlining its operating logic and overall architecture. Section VI discusses the validation process, based on comparisons with both

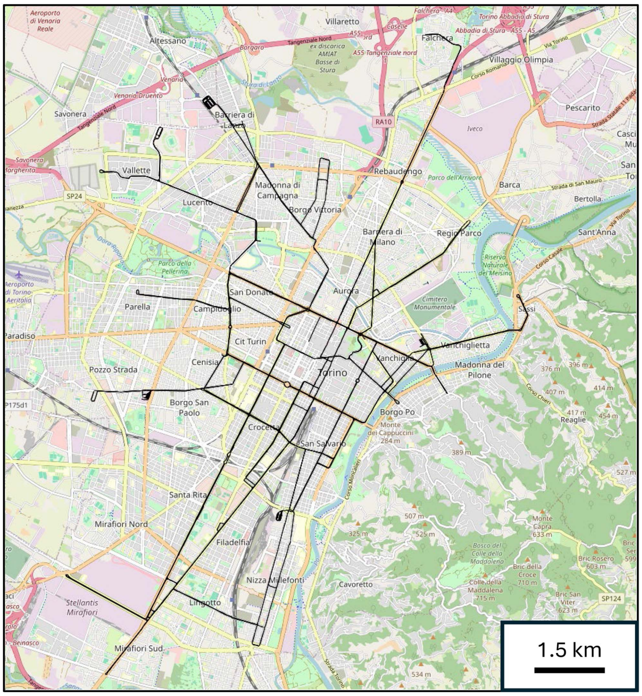

Fig. 1. Map of the tramway of Turin (map data from OpenStreetMap [20]).

simulation and field measurement results. Finally, Section VII concludes this article.

A. Mathematical Notation

In the following, a consistent notation is adopted to improve clarity. Matrices and arrays are denoted in boldface (e.g., $\mathbf{A}$), whereas scalars are expressed in italic (e.g., ρ). This convention is applied throughout this article to facilitate the distinction between different mathematical objects and to ensure the readability of the presented formulations.

II. UTES in Turin

Fig. 1 provides a picture of the tramways of Turin, characterized by a rail system longer than 180 km, 20 substations, and currently with more than 130 running trams.

Fig. 2 depicts the building blocks of the Turin tramway, providing pictures for the main components described as follows.

In the substations, a double secondary transformer steps the voltage down from 22 kV ac to 470 V ac, feeding a 12-pulse rectifier that produces a nominal dc output of 600 V. A switchgear houses the extra-rapid dc circuit breakers that protect the lines that feed the dc network. The circuit breakers' overcurrent settings range from 3000 to 4500 A.

The series of the positive cable, the copper bar interconnector, and the feeder cable interconnect the substations with the OCS, which is divided into 49 zones. Each zone is electrically separated from the others through insulation joints. Currently, a zone is fed by only one substation at a time. The OCS and positive feeder cables form a meshed network. Negative cables carry the return current to the rectifier by connecting it to the running rails. While the OCS is segmented into zones, the rails and negative cables form a unified, city-wide meshed network. The negative cables are kept separate from the substation grounding system to minimize stray currents, which are caused by the nonperfect insulation of the rail with respect to ground. In Turin's tram network, the positive feeder and negative cables have typical cross-sectional areas of $240\,\mathrm{mm}^2$, $500\,\mathrm{mm}^2$, and $1000\,\mathrm{mm}^2$, while the OCS has a cross-section of $95\,\mathrm{mm}^2$.

The network may be configured in various ways through two main approaches: remotely, by operating substation switches to manage individual zones, or locally, by modifying the copper junctions distributed across the network. The status of the circuit breaker and copper bar interconnections define the zones fed by each substation.

III. Electrical Models of the UTES Building Blocks

This section describes the electrical model of each network element described in Section II, which are the devices in the substations, the cable and overhead lines, and the trams. Moreover, since the software can also simulate fault scenarios, the model of an Earth fault along the line was developed.

A. Cables, OCS, and Rails

Each positive cable, feed cable, and overhead line of the OCS is modeled with a resistance. Its value is computed considering the resistivity of the conductor material (ρ), its length (L), and its cross-section (S) as reported in the following equation:

$$R = \rho \cdot L/S. \tag{1}$$

Setting the simulation options, the user can choose to model or neglect negative cables and rails. Including them means having a more accurate electrical model at the expense of a greater computational cost.

If explicitly considered, negative cables are modeled as the positive ones, while the rails are represented through a pi-model, where the shunt conductances represent the stray currents injected into the soil. The rail longitudinal resistance is computed through (1), while the total rail shunt conductance per unit length can be specified by the User. The default value is $0.8\,\mathrm{mS/km}$ [21].

If neglected, negative cables and rails are modeled as a unique ground node.

B. Substations

The transformer rectifier, the circuit breaker, and if present, the copper bar interconnector, are modeled with a Thevenin equivalent, formed by an ideal voltage generator and a resistance connected in series. The user can specify these parameters. The default values are 635 V and $16.7\,\mathrm{m}\Omega$, respectively [21]. Each substation contains multiple generators, one dedicated to each zone it supplies. The positive terminal of a generator is interconnected to the node of the first positive cable used to feed a substation. Considering the negative terminal, all generators within a substation are linked to a single, unique substation

This article has been accepted for inclusion in a future issue of this journal. Content is final as presented, with the exception of pagination.

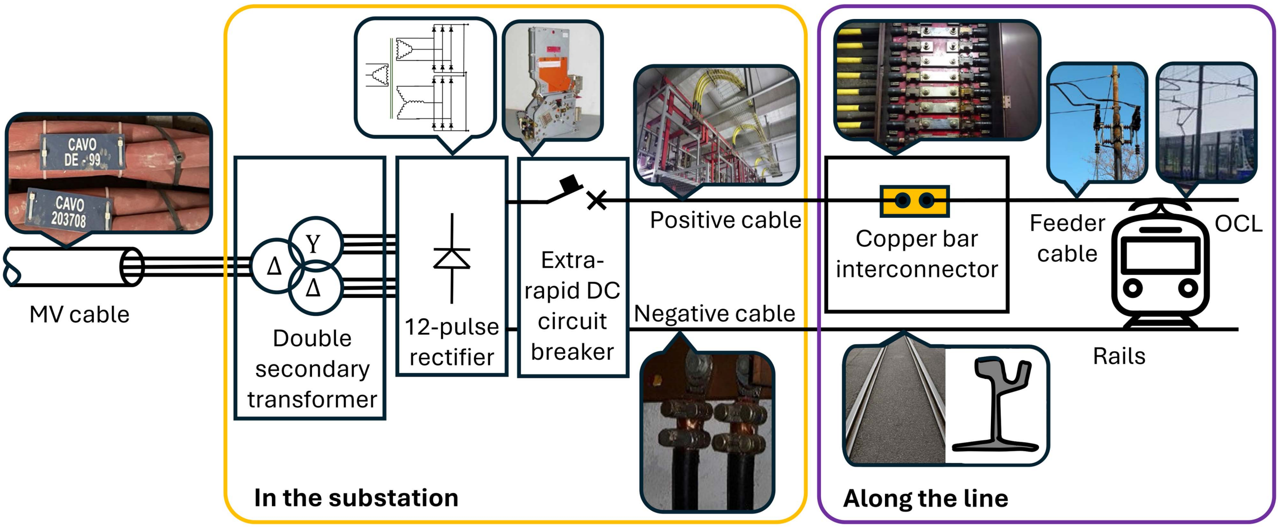

Fig. 2. Building blocks of the Turin UTES.

negative node. If tracks (and their corresponding negative cables) are modeled, all negative cables arriving at the substation are also connected to this node. In the absence of tracks in the model, the substation negative node serves as the ground node, shared among all substations across the city.

C. Copper Bar Interconnectors

Each copper bar interconnection is modeled as an ideal connection. Due to their small length (typically, around 20 cm), they impact the calculation only in defining the network topology.

D. Electric Public Transport Vehicles

Examples of EPTVs are trams or trolley-buses. As noted in the introduction, the simulator is intended to analyze steady-state conditions for grid and energy studies, either through a single scenario (e.g., the most critical time instant) or through a sequence of scenarios (e.g., to monitor in a quasi real-time manner the network or compare the absorbed current along a specific path for predictive maintenance purposes). The analysis of transient phenomena lies outside the scope of this study. For this reason, an EPTV can be easily represented by an ideal current source, whose set value corresponds to the absorbed current. In the case of regenerative braking, the numerical value is negative. The terminals of each current source are interconnected with a point of the OCS and a point of the rails. If the rails are not explicitly modeled, all the EPTVs are connected to the common ground node.

To simulate a sequence of steady-state events, the generator's current value can be updated using a dedicated machine learning algorithm that estimates the absorbed current based on the vehicle's position time series (latitude and longitude) [22]. An alternative approach, currently under development, involves the integration of an on-board smart meter to directly measure the absorbed current of the vehicle and transmit the data to a dedicated database [23].

Geometrically, EPTVs are defined as points. If an existing electrical node is located within a 1-m radius of the EPTV position, the EPTV is linked to that node. If no such node is found, the EPTV point is projected onto the nearest overhead contact line. This line is then split in two, creating a new node at the point closest to the EPTV position. The EPTV is subsequently connected to this newly created node.

E. Faults

A fault is modeled as a resistance that interconnects the OCS with the ground node or with tracks if they are explicitly modeled. The user can specify the fault resistance value. The default value is 0 Ω, i.e., the resistance of a bolted short circuit. Multifault scenarios can be modeled, inserting an arbitrary number of faults. The position of the fault is defined following the procedure adopted to locate trams. The unique difference is that a fault can be placed on the OCS but also on a positive or feeder cable.

IV. Electrical Circuit Solver

The solver computes the current in all the branches and the voltage in all the nodes of the UTES, using the nodal-analysis method in its matrix form [24].

Considering a network where the number of nodes is N and the number of branches is B, the method requires the following:

1) build the edge conductance matrix $\mathbf{G} = \{g_{ik}\} \in \mathbb{R}^{B,B}$. The matrix is diagonal and each entry $g_{i,i}$ is the total conductance of the ith branch;
2) build the voltage source array $\mathbf{v_s} = \{v_{s_i}\} \in \mathbb{R}^{B,1}$. The entry v_{s_i} represents the voltage imposed by the voltage source of the ith branch, in series with the branch conductance. The ideal voltage source used in the model

of substations feeding active zones described in Section III-B are the only nonzero entries of this array;

3) build the current source array $\mathbf{j_s} = \{j_{s_i}\} \in \mathbb{R}^{B,1}$. The entry j_{s_i} represents the current imposed by the current source of the ith branch, in parallel to the branch conductance. The ideal current generator described in Section III-D are the only nonzero entries of this array;
4) build the reduced incidence matrix $\mathbf{A} = \{a_{ij}\} \in \mathbb{R}^{N-1,B}$. The entry $a_{i,j}$ is: 1 if the jth branch exits the ith node; -1 if the jth branch enters the ith node; 0 otherwise;
5) compute the nodal admittance matrix $\mathbf{Y_n} \in \mathbb{R}^{N-1,N-1}$, as shown in (2)

$$\mathbf{Y_n} = \mathbf{A}\mathbf{G}\mathbf{A}^\mathbf{T} \tag{2}$$

6) solve the matrix (3)

$$\mathbf{Y_n}\mathbf{e} = \mathbf{i_s} \tag{3}$$

where
$\mathbf{e} = \{e_i\} \in \mathbb{R}^{N-1}$ is the unknown nodal voltage array. The entry e_i is the voltage between the ith node and the reference (ground) node;
and $\mathbf{i_s}$ is defined by (4)

$$\mathbf{i_s} = \mathbf{A}\mathbf{G}\mathbf{v_s} - \mathbf{A}\mathbf{j_s} \tag{4}$$

7) solve the matrix (5)

$$\mathbf{v} = \mathbf{A}^\mathbf{T}\mathbf{e} \tag{5}$$

where
$\mathbf{v} = \{v_i\} \in \mathbb{R}^{N-1}$ is the unknown branch voltage array. The v_i entry is the voltage drop in the ith branch.
8) solve the matrix (6)

$$\mathbf{j} = \mathbf{G}(\mathbf{v} - \mathbf{v_s}) + \mathbf{j_s} \tag{6}$$

where
$\mathbf{j} = \{j_i\} \in \mathbb{R}^{N-1}$ is the unknown branch current array. The j_i entry is the current flowing in the ith branch.

V. Turin Tram Network Simulator

Fig. 3 summarizes the main steps of the TTN-S. The grey areas describe the procedure to build the network topology and compute the electrical parameters described in Section III, in case only the geometrical representation of the UTES is available.

This procedure was mandatory because the data provided by Infra.To, the company managing the UTES infrastructure, was originally stored in an Autodesk DWG drawing file. Moreover, as software like AutoCAD allows us to draw large portions of the network quickly and easily, Infra.To technicians requested that the software can support this importing process also in the future. The software was implemented to overcome the inaccuracies often present in drawings that prevent having a reliable electric model. For example, two distinct points are considered the same electrical nodes if their distance is under the threshold ϵ, whose default value is 2 cm. Vice-versa, the network topology may be incorrect.

In case the UTES infrastructure is unchanged, it is possible to immediately import the last recent model, where the topological and electrical properties of the network are already properly organized (purple area).

In the green area, the steps to define the scenario under analysis are presented. A scenario can be built by specifying the status of the switches, drawing the copper bar interconnectors, selecting the position and the absorbed current of each EPTV, and selecting the position and the resistance of ground faults.

Finally, the electrical network solver described in Section IV is launched to compute the current in all the branches and the voltages of all the nodes. Only the active zones (i.e., those with at least an EPTV or a fault) are considered. An example of visualization of the results is reported in Fig. 4.

In the first developed software prototype, for ease of use and to avoid compatibility issues, the system is organized as a multicontainer Docker application, orchestrated with Docker Compose [25]. Fig. 5 reports a graphical representation of its services. For the development of the proposed tool, only free and open-source software was employed. Vice-versa, the first prototypal version of TTN-S is not publicly released.

The list of services (i.e., containers) included in the application are depicted in light blue. They are as follows.

1) App, which is a CherryPy server that hosts the simulator.
2) Tomcat, which is an Apache Tomcat server that hosts both the GeoServer and MapStore applications, which are distributed as web application resource files [26]. GeoServer is an open-source software server that allows us to share and edit geospatial data. MapStore is an open-source WebGIS framework that allows us to create, manage and share maps, integrating remote content from providers, such as Google Maps, OpenStreetMap, Bing, and other servers compliant to OGC standards.
3) DB, a PostGIS database that stores all the layers published in GeoServer [27]. PostGIS is a spatial database extension for the object-relational database PostgreSQL, which enables it to store data for GIS.
4) Mapstore DB, a PostgreSQL database that stores the configuration of MapStore, including both users and maps [28].

From the point of view of communications, the containers are all inside a Docker network that allows them to reference each other using service names as host names. Access is provided directly to the internal container ports. In addition, each container exposes some ports that are mapped to host ports, which are accessible from outside the Docker network (to allow access from the browser).

As for data storage, each container mounts a Docker volume that allows the persistence of critical data beyond the life cycle of the containers themselves.

VI. Model Validation

The developed model was validated by comparing an independently developed circuit model implemented in LTspice (see Section VI-A) and with experimental measurements (see Section VI-B), following the principles of the technical specification TS 50641-2 [29].

This dual approach ensures robustness by cross-verifying the outcomes obtained from the simulation software. Furthermore,

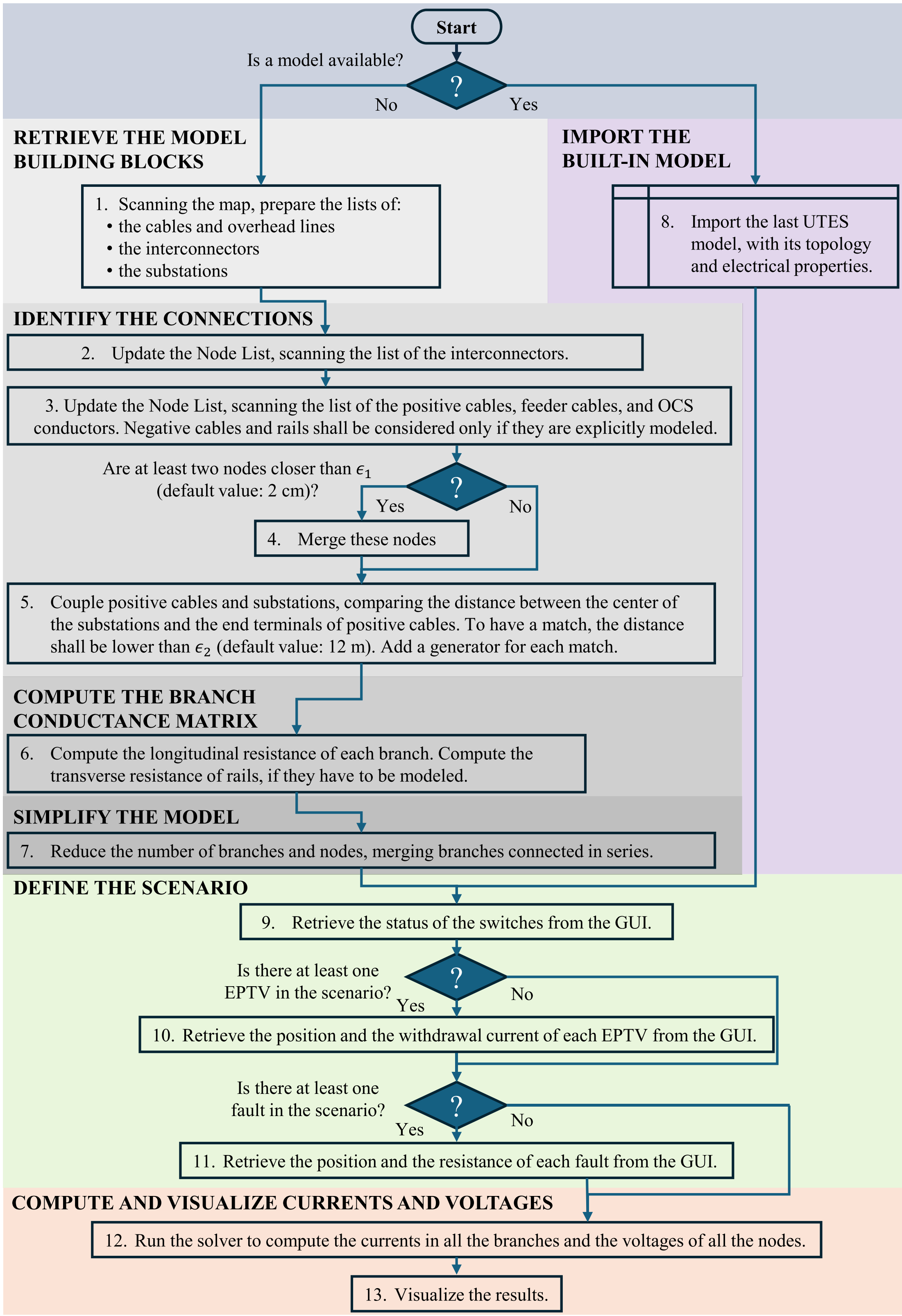

Fig. 3. Flowchart with the main steps of the software.

This article has been accepted for inclusion in a future issue of this journal. Content is final as presented, with the exception of pagination.

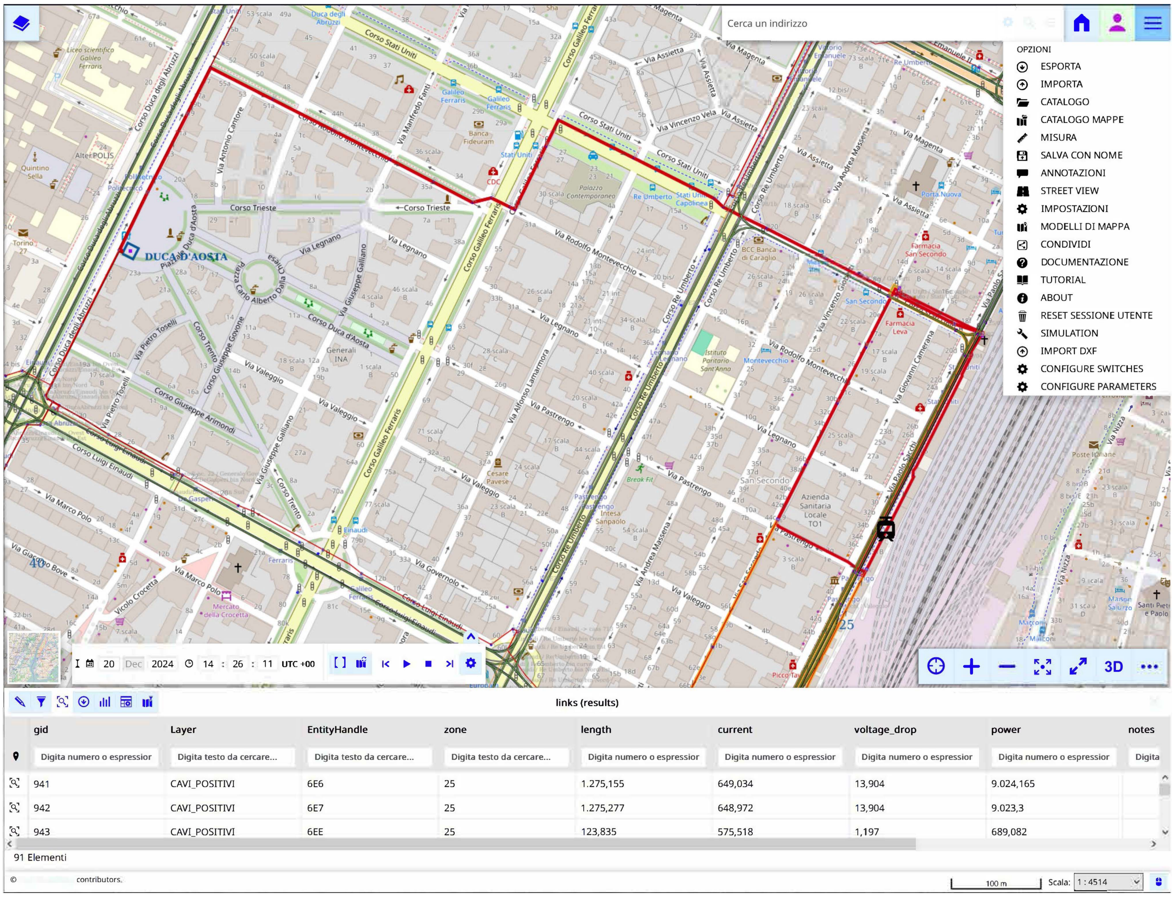

Fig. 4. TTN-S screen that shows the simulation results. The current flowing is marked in red. The highest the line width, the highest the current magnitude.

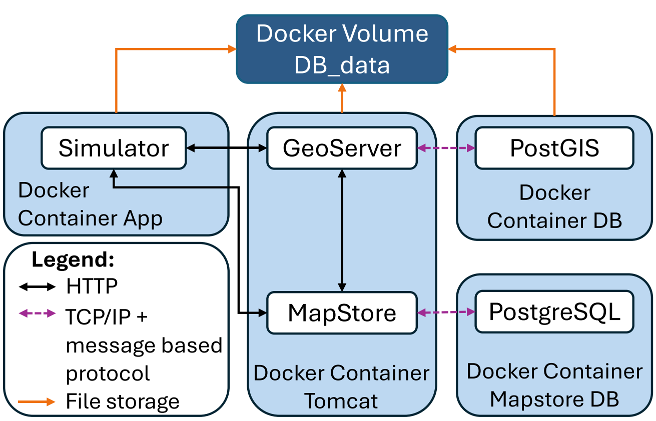

Fig. 5. Application architecture.

this approach demonstrates the capability of the simulation software to reliably model the tramway network's electrical behavior under various conditions.

A. Comparison With LTspice

The validation against the circuit model required manually constructing equivalent circuits representing normal operating scenarios (with trams absorbing specific currents) and fault conditions. LTspice was chosen for this task as it is available for free and easy to use [30].

In particular, the circuital model of the electric zone 25 was implemented. Each element of the UTES was constructed as described in Section III.

A normally operated UTES scenario was executed, with a tram circulating. Moreover, another scenario was considered, where a ground fault occurs.

In both cases, the differences between the currents in all the branches and the voltages in all the nodes are negligible (always lower than 0.01%).

This test verified that the software could correctly generate the equivalent electrical circuit based on the geometric representation and that the solver accurately calculated currents and voltages.

B. Comparison With the Results of the Field Measurement Campaign

To validate the model against experimental measurements, it was necessary to record the position of the vehicle, the pantograph voltage, and the current absorbed by a tram operating in a zone of the UTES where no other vehicle was circulating. Having a controlled test, i.e., governing the test parameters that can affect the voltage and current distribution, was mandatory

This article has been accepted for inclusion in a future issue of this journal. Content is final as presented, with the exception of pagination.

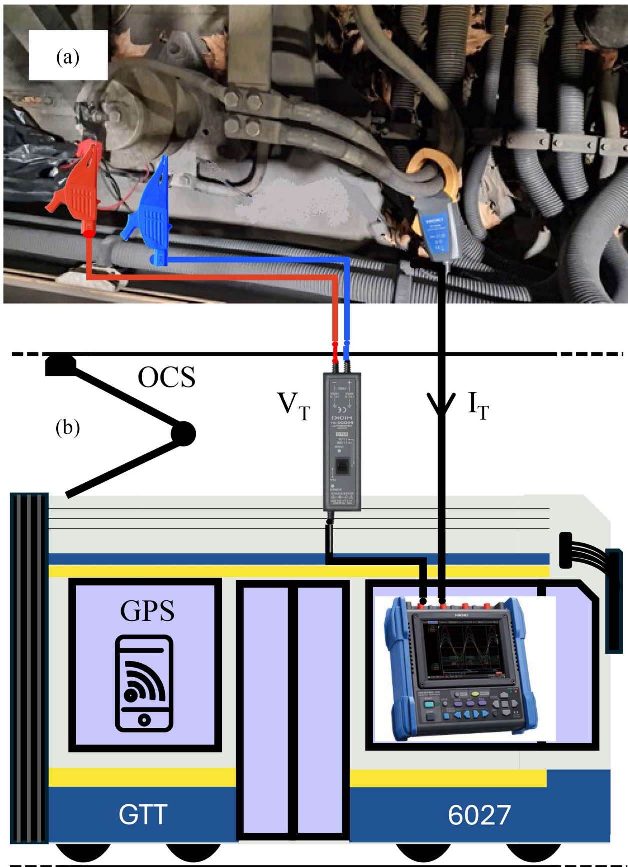

Fig. 6. Measurement setup. (a) Top view. (b) Side view.

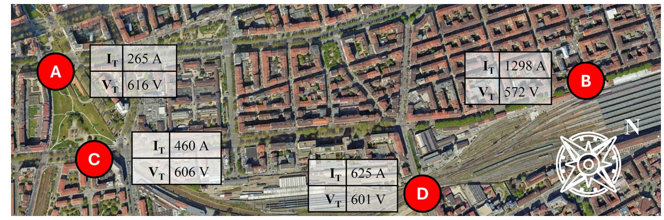

Fig. 7. Positions of the tram considered to validate the models.

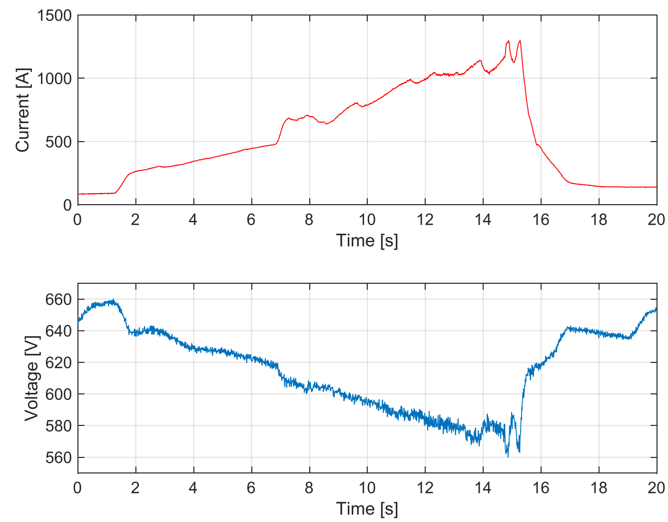

Fig. 8. Example of measured current and voltage signals.

to properly compare the results of the field measurement and of the TTN-S. For this reason, the field measurement campaign was carried out at night, operating the tram 6027 on a 25 km route where two distinct electrical zones of the UTES can be identified (zone 25 and 28).

Fig. 6 reports the field measurement setup. The position of the vehicle was measured through the GPS signal of a smartphone with an accuracy of 7 m. On the top of the vehicle, the current and voltage probes were installed to measure the current absorbed by the tram (I_T) and the voltage at the pantograph (V_T), respectively. The signals were transferred through two cables inside the cabin, where the HIOKI MR8880 High-speed recorder registered them with a sampling period of 10 ms. All the instruments were calibrated to measure null quantities when the pantograph was lowered. The errors of current and voltage signals were $\pm$ 2.0 % of the reading value $\pm$ 48 A and $\pm$ 2.0 % of the reading value $\pm$ 30 V, respectively.

The maximum and minimum recorded currents are 1298 A and -324 A, in acceleration and breaking events, respectively. A negative current value stands for regenerative braking. The maximum and minimum measured voltages are 763 V and 363 V. These values depend on the distance from the substation, the acceleration profile, the status of charge of the onboard capacitors of the LC filter, and the presence of short insulating sections that separate adjacent electrical zones.

Analyzing the voltage when the tram is stopped, it is possible to measure the no-load output voltage of the converter in the substation, which is 662.5 V for both the electric zones.

Fig. 7 reports 4 positions of the tram, together with the measured current and voltage. Fig. 8 represents the current and voltage signals measured during the acceleration event in point B of Fig. 7, as an example.

These 4 scenarios were implemented with the TTN-S, setting the measured position and absorbed current as input. The voltage of the OCS at the vehicle's location calculated by the TTN-S was compared with the measured value and the computed values obtained using the circuital model implemented in LTspice, manually built to ensure that the software constructs the system correctly and automatically. Table II reports the comparison results. Once again, TTN-S and LTspice provide practically identical results. Therefore, it can be concluded that TTN-S can properly identify the connections among the elements, and write and solve the equations described in Section IV. The maximum error ΔE_T calculated considering the measured values as references is 6.0%. The difference can be explained considering that the return circuit was modeled in neither TTN-S nor the LTspice circuit, due to the lack of full information on the Turin dataset. Even if a data polishing activity must be conducted to improve the quality of the model, the differences between the measured and calculated quantities fall within the acceptable threshold, considering the scope of the DT and the error of measurement.

This article has been accepted for inclusion in a future issue of this journal. Content is final as presented, with the exception of pagination.

TABLE II
FOR THE TRAM IN THE POSITION P WHILE DRAWING THE MEASURED CURRENT I_T, ΔE_T, AND ΔE_{LTS} REPRESENT THE PERCENTAGE ERRORS BETWEEN THE VOLTAGE AT THE PANTOGRAPH COMPUTED BY THE TTN-S ($V_{\text{TTN-S}}$), THE MEASURED ONE (V_T), AND THE ONE COMPUTED WITH LTSPICE (V_{LTS}), RESPECTIVELY

P -	I_T [A]	V_T [V]	$V_{\text{TTN-S}}$ [V]	V_{LTS} [V]	ΔE_T [%]	ΔE_{LTS} [%]
A	265	616	647	647	5.1	0.0
B	1298	572	607	607	6.0	0.0
C	460	606	638	638	5.3	0.0
D	625	601	632	632	5.2	0.0

In evaluating computational time, two phases should be distinguished. The first concerns network construction, which is required in both LTSpice and the proposed software; however, in LTSpice this phase is considerably more time-consuming and prone to errors. The second concerns the calculation of currents and voltages for a single simulation, the duration of which is limited to only a few seconds.

VII. CONCLUSION

This study describes a methodology to implement a model of a UTES based on geographical maps, and the developed model for the infrastructure in Turin, Italy. The developed application is web-based and georeferenced, and it is one of the main building blocks to implement a DT of the Turin tramway. It allows us to visualize and explore the status of each element in the model and computes the current in all the lines and the voltages at all the nodes both in normal operating service and in fault condition. The model was validated through the comparison with data collected on a field measurement campaign and computed by solving an equivalent electrical circuit through LTspice, an open-source software. The errors between the calculated results are negligible, while those considering the field measurement as a reference are lower than 6%, probably due to the incompleteness of the negative circuits dataset and the error of measurement. A data polishing activity on the negative circuits must be conducted to get better results, even if this error magnitude can be considered satisfactory.

Future work will focus on advancing DT implementation by developing an onboard smart meter to measure the electrical current absorbed by each tram in the network, and by restructuring the platform to enable seamless integration of the measured data into the model. This modification will ensure that the system can dynamically utilize real-world quasi-real-time data, improving its predictive performance and adaptability to diverse operational scenarios. The proposed software represents a versatile platform with both scientific and industrial value. It supports the development of optimization algorithms, predictive maintenance strategies, and studies on the impact of electric vehicle charging on dc traction networks, while also serving as a practical decision-support tool to enhance efficiency and resilience in tramway infrastructures.

ACKNOWLEDGMENT

The authors would like to thank “Gruppo Torinese Trasporti (GTT S.p.A.)” and “Infra.To - Infrastrutture per la mobilità” for their valuable and constructive suggestions during the planning and development of this research work, particularly Simone Baj, Felice Calamusa, Marianna Costa, Salvatore Gaudiello, Ivo Giammò, and Roberto Rizzoli. They also would like to thank the students Francesco Barlocco and Davide Speziale for their help. This article reflects only the authors’ views and opinions and the Ministry cannot be considered responsible for them.

REFERENCES

[1] European Commission, Communication from the Commission to the European Parliament, the Council, the European Economic and Social Committee and the Committee of the Regions, Eds. *The new EU Urban Mobility Framework, Brussels, Belgium, COM*, 811 final, Dec. 2021.
[2] E. Pons, P. Colella, R. Rizzoli, and R. Tommasini, “Optimization of digital overcurrent protection settings in dc urban light railway systems,” *IEEE Trans. Ind. Appl.*, vol. 55, no. 4, pp. 3437–3444, Apr. 2019.
[3] F. Tao, H. Zhang, A. Liu, and A. Y. C. Nee, “Digital twin in industry: State-of-the-art,” *IEEE Trans. Ind. Informat.*, vol. 15, no. 4, pp. 2405–2415, Apr. 2019.
[4] R. Barbone, R. Mandrioli, M. Ricco, R. F. Paternost, V. Cirimele, and G. Grandi, “Novel multi-vehicle motion-based model of trolleybus grids towards smarter urban mobility,” *Electronics*, vol. 11, no. 6, pp. 1–23, 2022, doi: 10.3390/electronics11060915.
[5] D. Yang, A. Mahmood, S. A. Hassan, and M. Gidlund, “Guest editorial: Industrial IoT and sensor networks in 5G-and-beyond wireless communication,” *IEEE Trans. Ind. Informat.*, vol. 18, no. 6, pp. 4118–4121, Jun. 2022.
[6] E. Sisinni, A. Saifullah, S. Han, U. Jennehag, and M. Gidlund, “Industrial Internet of Things: Challenges, opportunities, and directions,” *IEEE Trans. Ind. Informat.*, vol. 14, no. 11, pp. 4724–4734, Nov. 2018.
[7] M. V. Moreno et al., “Applicability of Big Data techniques to smart cities deployments,” *IEEE Trans. Ind. Informat.*, vol. 13, no. 2, pp. 800–809, Feb. 2017.
[8] Z. Wei, K. Liu, X. Liu, Y. Li, L. Du, and F. Gao, “Multilevel data-driven battery management: From internal sensing to big data utilization,” *IEEE Trans. Transport. Electrific.*, vol. 9, no. 4, pp. 4805–4823, Apr. 2023.
[9] A. De Benedictis, F. Flammini, N. Mazzocca, A. Somma, and F. Vitale, “Digital twins for anomaly detection in the industrial Internet of Things: Conceptual architecture and proof-of-concept,” *IEEE Trans. Ind. Informat.*, vol. 19, no. 12, pp. 11553–11563, Dec. 2023.
[10] M. Prussi, A. F. Cota, L. Laveneziana, G. Chiantera, and P. Guglielmi, “Electric vehicle charging from tramway infrastructure: A new concept and the turin case study,” *Energies*, vol. 17, no. 5, pp. 1–15, 2024, doi: 10.3390/en17050984.
[11] P. Franzese et al., “Fast DC charging infrastructures for electric vehicles: Overview of technologies, standards, and challenges,” *IEEE Trans. Transport. Electrific.*, vol. 9, no. 3, pp. 3780–3800, Sep. 2023.
[12] “GTT — gtt.to.it.” Accessed: Nov. 8, 2024. [Online]. Available: https://www.gtt.to.it/cms/
[13] “Infra.to | infrastrutture per la mobilità; — infrato.it.” Accessed: Nov. 8, 2024. [Online]. Available: https://www.infrato.it/
[14] “Geospatial track modeling—etrax$^{\text{TM}}$—railways | transportation—etap,” Default, 2016. [Online]. Available: https://etap.com/product/geospatial-track-modeling
[15] “Fabel simulation software—Enotrac,” *Enotrac*, 2025. [Online]. Available: https://enotrac.com/en/products/fabel/
[16] “Openpowernet—Simulation software for railway power supply systems,” *Openpowernet.de*, 2025. [Online]. Available: https://www.openpowernet.de/
[17] “Traction power networks are the focus of tomorrow’s mobility,” Siemens Mobility Global, 2025. [Online]. Available: https://www.mobility.siemens.com/global/en/portfolio/digital-solutions-software/infrastructure/rail-electrification/sidytrac.html
[18] “Home - signon,” SIGNON, 2024. [Online]. Available: https://signon-suite.com/en/

[19] A. Nyman, "Tts/simon power log—A simulation tool for evaluating electrical train power supply systems," *WIT Trans. Built Environ.*, vol. 37, pp. 1–10, 1998, doi: 10.2495/CR980411.
[20] "Copyright and License—Openstreetmap.org." Accessed: Jan. 3, 2025. [Online]. Available: openstreetmap.org/copyright
[21] E. Pons, R. Tommasini, and P. Colella, "Fault current detection and dangerous voltages in dc urban rail traction systems," *IEEE Trans. Ind. Appl.*, vol. 53, no. 4, pp. 4109–4115, Apr. 2017.
[22] P. Colella et al., "Digital twin implementation for urban tram systems: A data-driven model for estimating traction current," in *Proc. Int. Conf. Environ. Elect. Eng.*, 2025, pp. 1–6, doi: 10.1109/eeeic/icpseurope64998.2025.11169175.
[23] D. Giordano et al., "Voltage divider design for dc traction in tramway networks," in *Proc. Int. Conf. Environ. Elect. Eng.*, 2025, pp. 1–5, doi: 10.1109/eeeic/icpseurope64998.2025.11169159.
[24] C. A. Desoer, E. S. Kuh, and G. Biorci, in *Fondamenti Di Teoria Dei Circuiti*, Milano, Italy: FrancoAngeli, 1995.
[25] "What is Docker?—docs.docker.com." Accessed: Nov. 13, 2024. [Online]. Available: https://docs.docker.com/get-started/docker-overview/
[26] A. T. Project, "Apache Tomcat—tomcat.apache.org." Accessed: Nov. 13, 2024. [Online]. Available: https://tomcat.apache.org/
[27] "GeoServer 2.26.x User Manual—docs.geoserver.org." Accessed: Nov. 13, 2024. [Online]. Available: https://docs.geoserver.org/stable/en/user/
[28] "Quick Setup and Run—MapStore—docs.mapstore.geosolutionsgroup.com." Accessed: Nov. 13, 2024. [Online]. Available: https://docs.mapstore.geosolutionsgroup.com/en/v2024.02.01/developer-guide/
[29] Fixed Installations for Railway Applications—Requirements for the Validation of Simulation Tools Used for the Design of Electric Traction Power Supply Systems—Part 2: Specific DC Urban Case, PD CLC/TS 50641-2:2024, 2024.
[30] Accessed: Nov. 22, 2024. [Online]. Available: https://www.analog.com/en/resources/design-tools-and-calculators/ltspice-simulator.html

Pietro Colella (Member, IEEE) received the M.Sc. and Ph.D. degrees in electrical engineering from Politecnico di Torino, Turin, Italy, in 2012 and 2016, respectively.

He is currently an Associate Professor with Politecnico di Torino, where he teaches courses in electrical installations. He is currently a Principal Investigator for several industrial and publicly funded research projects. His research interests include power systems, electricity markets, traction electrification, clustering and artificial intelligence algorithms applied to power systems, and electrical safety.

Dr. Colella is also a member of AEIT, the Italian Association of Electrical, Electronics, Automation, Information and Communication Technology.

Enrico Pons (Senior Member, IEEE) received the master's degree in electrical engineering and the Ph.D. degree in industrial safety and risk analysis from Politecnico di Torino, Turin, Italy, in 2004 and 2008, respectively.

He is currently an Associate Professor with Politecnico di Torino, where he teaches electrical installations. His research interests include complexity in energy systems, power systems security, complex network methodologies for the analysis of power systems vulnerability, real-time simulation of power systems, integration of renewable generation in distribution networks, smart metering, traction electrification systems, and electrical safety.